解 説

# Hardware and Control Concept for an Experimental Bipedal Robot with Joint Torque Sensors

Christian Ott\*, Oliver Eiberger\*, Johannes Englsberger\*, Maximo A. Roa\* and Alin Albu-Schäffer\*

\*German Aerospace Center (DLR e.V.)

#### 1. Introduction

Research on bipedal walking is driven by the vision of humanoid robotic servants for the society of the future. Besides the human form, bipedal locomotion offers the possibility to step over small obstacles and stairs and allows for a relatively small support area.

Active control of the zero-moment-point (ZMP) [15] by measuring the contact forces at the feet and precisely controlling the motion of the robot has been shown to be an effective paradigm of stabilizing walking motions of bipedal robots [2] [6]. In the design of humanoid robots that utilize this control approach the precision of the position controllers plays an important role [7] $\sim$  [9] [12] [14].

Joint torque sensing and control allows sensitive compliance and impedance control [10], but requires additional instrumentation in the drive units. The humanoid robot CB [1] utilizes explicit joint torque sensing in a hydraulic actuation system. Serial elastic actuators also offer an indirect way of measuring the joint torque and were applied to bipedal walking in Ref. [13]. While these actuators allow for force control due to their low impedance characteristics, precise trajectory tracking becomes more difficult.

In this paper we present the hardware and control concepts for an electrically driven bipedal robot with integrated joint torque sensors (Fig. 1). The robot was designed as an experimental system for research on control aspects, including comparisons between strategies based on joint position or joint torque control.

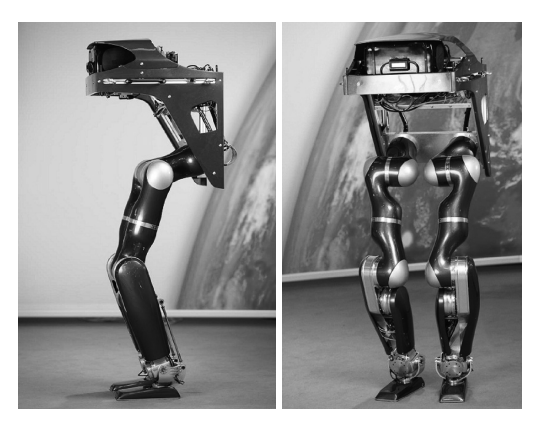


Fig. 1 DLR-Biped with torque controlled joints

# 2. Mechanical Design

# 2.1 Design Goal

In order to allow research on walking based on joint torque control, the robot should be equipped with joint torque sensors in all the joints. At the same time, the drive system should be stiff enough to allow comparisons with position based walking control algorithms. In order to keep the development time low, the drive units of the robot are based on the modular drives of the DLR-Lightweight-Robot-II [4]. Besides dynamic walking on flat floor, the robot should be able to climb stairs with a roughly defined step height of about  $10\sim20\,[\mathrm{cm}]$ .

# 2.2 Kinematics & Drive Units

For the leg kinematics, a non-redundant configurations with six degrees of freedom per leg was chosen (see **Fig. 2**). The kinematics of the three hip axes in a roll-pitch-roll configuration was adopted from the segments of the DLR-Lightweight-Robot-II, while the design of the lower leg required a customized design. In order to minimize the load on the first two hip axes it is beneficial to keep the distance between the legs small and to keep the total center-of-mass (COM) close to the rotation axis of the hip pitch axis. The first hip axis is tilted by an adjustable angle  $\alpha$  from the horizontal direction.

原 2012年3月5日

<sup>+-7-</sup> F: Bipedal Robot, Torque Control, Bipedal Walking \*P.O. Box 1116, 82234 Wessling, Germany

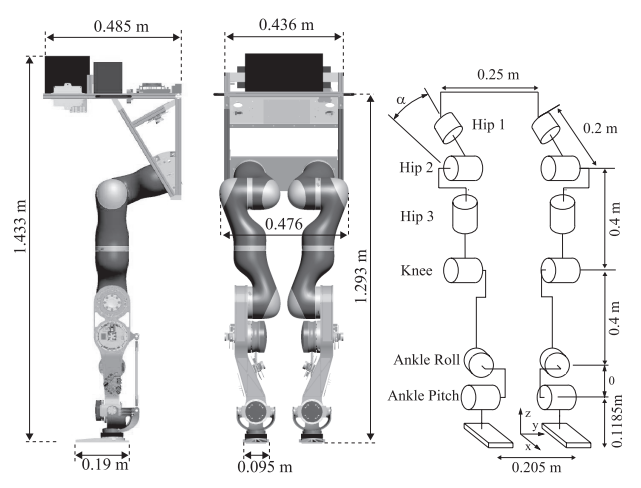


Fig. 2 Size of the DLR-Biped

A larger angle  $\alpha$  leads to a smaller load on the first axis during single support, but brings the joint configuration closer to a singular configuration when the first and third hip axes become parallel. In order to allow stepping on different stair sizes up to  $20 \, [\mathrm{cm}]$ , the angle  $\alpha$  is nominally set to  $20 \, [\mathrm{deg}]$ .

For the design of the lower leg, two powerful drive units for the knee and the ankle pitch axis are combined with a smaller motor for the ankle roll axis. The chosen configuration of a pitch-roll-pitch configuration for the knee and the ankle allows to keep the pitch axis of the ankle parallel to the ground. Since the pitch axis is mainly responsible for the forward motion, while the roll axis is mainly responsible for the lateral motion, the chosen joint configuration can be beneficial for large forward steps. In order to achieve a slim design in the ankle and to locate its mass as high as possible, the drive unit of the pitch axis is located in the lower leg just below the knee joint and is driving the joint axis with a rod connection (see Fig. 2). Moreover, in order to avoid collisions between the knee segments, the foot distance is chosen smaller than the hip distance.

In the current configuration, the contact area of each foot can be adapted via different adapter plates allowing for a minimal rectangular foot area of  $9.5 \times 19$  [cm]. In order to reduce shocks during touch-down, an additional thin damping layer was applied to the sole at the front and rear part.

Table 1 shows the maximum joint velocities and joint torque limits for the individual joints. These limitations were evaluated in dynamics simulations using OpenHRP3. As benchmark tasks, dynamic walking motions for walking speeds up to 1.35 [km/h] and squat

Table 1 Drive units

| Joint   | Motor     | Gear  | $\dot{q}_{\mathrm{max}}$ | $	au_{ m max}$ | $q_{\min}$ | $q_{\rm max}$ |
|---------|-----------|-------|--------------------------|----------------|------------|---------------|
|         | Power [W] | Ratio | $[^{\circ}/\mathrm{s}]$  | [Nm]           | [°]        | [°]           |
| Hip 1   | 270       | 160   | 120                      | 100            | -170       | 170           |
| Hip 2   | 270       | 160   | 120                      | 100            | -120       | 60            |
| Hip 3   | 270       | 100   | 180                      | 70             | -170       | 170           |
| Knee    | 450       | 160   | 110                      | 180            | -115       | 115           |
| Ankle R | 140       | 160   | 120                      | 50             | -20        | 20            |
| Ankle P | 450       | 160   | 110                      | 180            | -45        | 45            |

motions on one and two legs were performed.

The overall size of the robot is shown in Fig. 2. Including all the onboard power supply and computer system, the total weight of the robot is about  $m=53.5\,[\mathrm{kg}]$ , with  $8.2\,[\mathrm{kg}]$  for each upper leg and  $7.1\,[\mathrm{kg}]$  for each lower leg.

#### 2.3 Sensor System

The internal state of the robot can be measured by the motor position and joint torque sensors. In order to enable comparisons of bipedal walking controllers based on joint torque sensing with controllers based on admittance control, the robot is additionally equipped with two six-axis force/torque sensors in the feet.

For measuring the orientation of the trunk, the robot is equipped with an inertial measurement unit (IMU). Moreover, a stereo camera system was integrated to allow research on autonomous navigation.

The low level position and torque controllers in the drive units are executed in a sampling time of 0.33 [ms] and the joint data is transferred via a SERCOS II bus to an onboard control computer running under VxWorks in a sampling time of 1 [ms]. The force sensors and the IMU are accessed from the control computer via serial interfaces and allow sampling rates of 2 [ms] and 4 [ms], respectively. The stereo cameras are providing online vision data in a slower rate to an onboard computer running under Linux.

#### 3. Control

# 3.1 Torque based Balancing and Posture Control

In order to balance the bipedal robot against external disturbances, compliant motion control is useful. Our approach for balancing takes advantage of the integrated joint torque sensors, which allow a highly sensitive inner loop joint torque control [10].

Fig. 3 shows the structure of the torque based balancing and posture controller [11]. Given a desired equilibrium  $r_d$  for the COM position r and a desired orien-

380

Fig. 3 Overview of the balancing controller

tation  $\mathbf{R}_d$  of the trunk, we compute a desired wrench  $\mathbf{F}_d$  which we want to apply onto the robot at the COM according to a compliance control law, i.e.

$$\boldsymbol{F}_{d} = \begin{pmatrix} m\boldsymbol{g} \\ \boldsymbol{0} \end{pmatrix} - \boldsymbol{D} \begin{pmatrix} \dot{\boldsymbol{r}} \\ \boldsymbol{\omega} \end{pmatrix} - \begin{pmatrix} \boldsymbol{K}_{t}(\boldsymbol{r} - \boldsymbol{r}_{d}) \\ \boldsymbol{\tau}_{k}(\boldsymbol{R}, \boldsymbol{R}_{d}) \end{pmatrix}, \quad (1)$$

where R and  $\omega$  denote the orientation and the angular velocity of the trunk, which are both measured by the onboard IMU. Damping is implemented by the matrix D.  $K_t$  and  $\tau_k$  denote the translational stiffness and the torque from a virtual rotational spring between R and  $R_d$ .

This desired wrench  $\mathbf{F}_d$  is distributed to the supporting contact points at the feet. Therefore, we consider the mapping between the contact forces  $\mathbf{f}_C$  and the total wrench  $\mathbf{F}$  via the 'grasp matrix'  $\mathbf{G}$ , i.e.  $\mathbf{F} = \mathbf{G}\mathbf{f}_C$ . The desired contact forces  $\mathbf{f}_C$  are then computed based on a constrained minimization of the error  $||\mathbf{F} - \mathbf{F}_d||$ . Thereby, unilaterality constraints on the contact forces and friction cone constraints can be considered in the solution of the constrained optimization problem, which implies a limitation of the ZMP to the support polygon.

In order to realize the desired contact forces  $f_C$ , we summarize the contact forces at the right and left foot to the corresponding contact wrenches  $F_r$  and  $F_l$  and map these contact wrenches to corresponding joint torques  $\tau_d$ . For an exact implementation of this 'mapping', the whole multi-body robot dynamics should be considered. As a simpler solution, we can also consider only a kinetostatic mapping based on the relevant Jacobian matrices, which can be derived by considering the interaction of the isolated COM dynamics with the remaining multi-body dynamics [11]. This leads to

$$\boldsymbol{\tau}_d = \boldsymbol{J}_r^T \boldsymbol{F}_r + \boldsymbol{J}_l^T \boldsymbol{F}_l , \qquad (2)$$

where  $J_r$  and  $J_l$  denote the Jacobian matrices for the right and left foot with respect to the COM location r.

The resulting control scheme does not require any measurement of the contact forces at the feet, and can

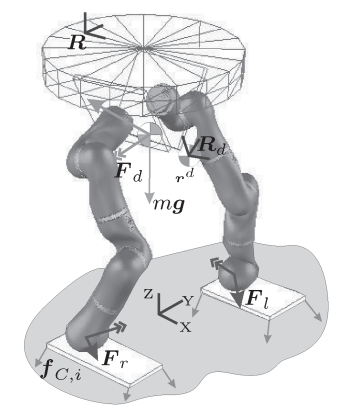




Fig. 4 Involved forces in the balancing controller

be made robust against uncertainties in the ground geometry by utilizing a state measurement based on the IMU data. **Fig. 4** shows an example in which the bipedal robot is balancing against external disturbances, while standing on an un-firm supporting area.

## 3.2 Walking Control

For walking control we follow an approach based on an underlying ZMP controller, which can be implemented either via joint position or torque control. Instead of a COM-ZMP pattern generator with an underlying feedback controller, our walking control approach from Ref. [3] aims at a feedback control law. Let us consider the widely used linear inverted pendulum dynamics  $\ddot{x} = \omega^2(x-p)$  with  $\omega$  as the time constant and p as the location of the ZMP. By utilizing the 'Capture Point' (CP)  $\xi = x + \dot{x}/\omega$  [5], at which the ZMP asymptotically stops the COM motion, the dynamics can be transformed into a system with block-diagonal structure

$$\dot{x} = -\omega(x - \xi) , \qquad (3)$$

$$\dot{\xi} = \omega(\xi - p) \ . \tag{4}$$

The basic idea of the controller design is to stabilize the unstable CP dynamics (4) with a feedback controller

$$p = 1/(1-k)\xi_d - k/(1-k)\xi$$
, (5)

while keeping the stable COM dynamics (3) unchanged. Choosing  $k = e^{\omega T}$  for a time parameter T allows to steer the CP to its desired value  $\xi_d$  until time T.

From the extension of (4) to the planar case describing lateral and sagittal motion, we can observe that by placing the ZMP at a certain point it is possible to steer the CP along a straight line (see Fig. 5). Given predefined footsteps, the planning of a reference trajectory for the CP thus requires only the planning of straight lines.

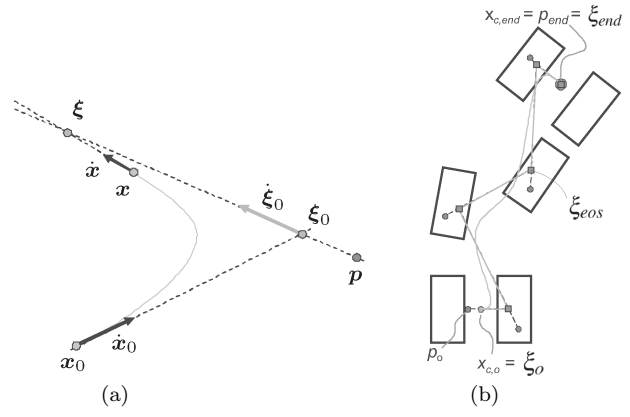


Fig. 5 Two-dimensional Capture Point shifting:
(a) basic shifting mechanism, (b) foot to foot shift

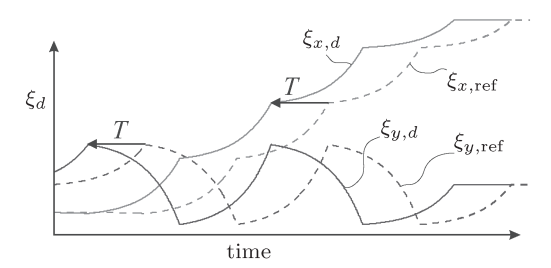


Fig. 6 Generation of the desired CP trajectories

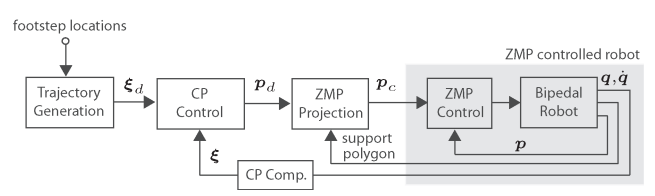


Fig. 7 Overview of the walking controller

The resulting reference trajectories are commanded to the CP controller (5) by considering the time parameter T related to the controller gain (see **Fig. 6**).

In order to ensure that the commanded ZMP stays within the current support polygon, a projection is required, which is performed preferably along the line connecting  $\xi$  and  $\xi_d$  (see Fig. 9 (a)). **Fig. 7** shows an overview of the walking controller.

The CP based walking controller lead in combination with an underlying position based ZMP controller to stable walking motions on flat ground for a step time of 0.8 [s] and step lengths up to about 20 [cm]. Fig. 8 shows experimental results of a forward walking experiment with a step size of 10 [cm]. Also, initial experiments on stairs showed promising results (Fig. 9).

# 4. Summary and Outlook

This article presented the design considerations and the basic control approaches for the DLR-Biped with

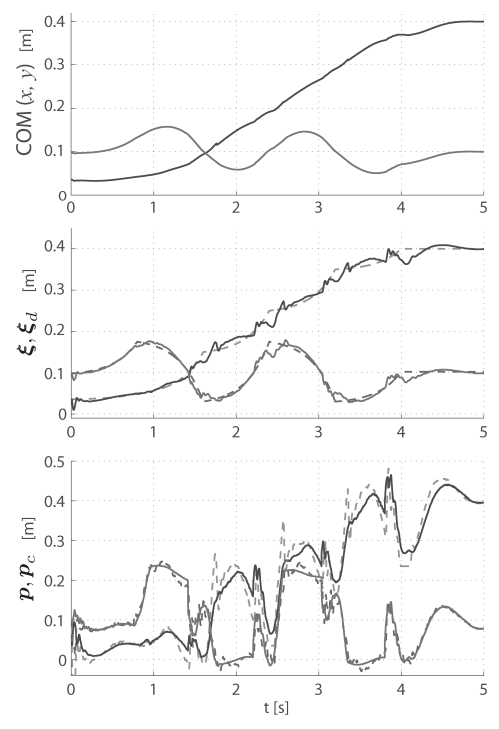


**Fig. 8** Experimental results. The upper two graphs show the COM and the CP, while the lower graph shows the ZMP in x and y direction

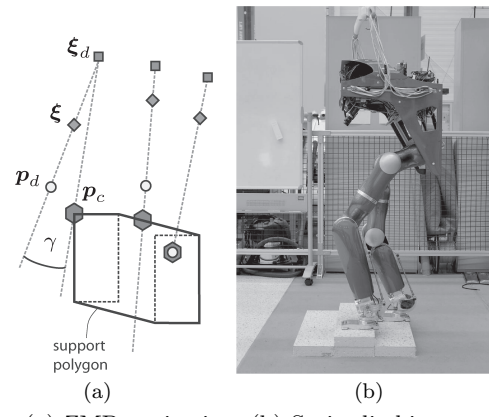


Fig. 9 (a) ZMP projection, (b) Stair climbing experiment

integrated joint torque sensors. Future work on the walking controller will aim at a generalization to more precise models of the robot dynamics including variations of the COM height. Moreover, the performance of the controller with an underlying torque based ZMP or force controller will be investigated.

**Acknowledgements** This research is partly supported by the Initiative and Networking Fund of the Helmholtz Association (VH-NG-808).

#### References

[1] G. Cheng, S.-H. Hyon, J. Morimoto, A. Ude, G. Colvin, W. Scroggin and S.C. Jacobsen: "Cb: A humanoid research

- platform for exploring neuroscience," IEEE-RAS International Conference on Humanoid Robots, 2006.
- [2] Y. Choi, D. Kim, Y. Oh and B.-J. You: "Posture/walking control for humanoid robot based on kinematic resolution of com jacobian with embedded motion," IEEE Transactions on Robotics, vol.23, no.6, pp.1285–1293, 2007.
- [3] J. Englsberger, C. Ott, M.A. Roa, A. Albu-Schäffer and G. Hirzinger: "Bipedal walking control based on capture point dynamics," IEEE/RSJ Int. Conference on Intelligent Robots and Systems, 2011.
- [4] G. Hirzinger, A. Albu-Schäffer, M. Hähnle, I. Schaefer and N. Sporer: "On a new generation of torque controlled lightweight robots," IEEE Int. Conf. on Robotics and Automation, pp.3356–3363, 2001.
- [5] S. Drakunov, J. Pratt, J. Carff and A. Goswami: "Capture point: A step toward humanoid push recovery," IEEE-RAS International Conference on Humanoid Robots, pp.200–207, 2006.
- [6] S. Kajita, M. Morisawa, K. Miura, S. Nakaoka, K. Harada, K. Kaneko, F. Kanehiro and K. Yokoi: "Biped walking stabilization based on linear inverted pendulum tracking," IEEE/RSJ Int. Conference on Intelligent Robots and Systems, pp.4489–4496, 2010.
- [7] K. Kaneko, F. Kanehiro, M. Morisawa, K. Miura, S. Nakaokaand and S. Kajita: "Cybernetic human hrp-4c," Proc. 9th IEEE-RAS International Conference on Humanoid Robots, pp.7–14, 2009.

[8] S. Lohmeier, T. Buschmann and H. Ulbrich: "System design and control of anthropomorphic walking robot lola," IEEE/ASME Transactions on Mechatronics, vol.14, no.6, pp.658-666, 2009.

Alin Albu-Schäffer

Maximo A. Roa

- [9] Y. Ogura, H. Aikawa, K. Shimomura, H. Kondo, A. Morishima, H.O. Lim and A. Takanishi: "Development of a new humanoid robot wabian-2," IEEE Int. Conf. on Robotics and Automation, pp.76–81, 2006.
- [10] C. Ott, A. Albu-Schäffer, A. Kugi and Gerd Hirzinger: "On the passivity based impedance control of flexible joint robots," IEEE Transactions on Robotics, vol.24, no.2, pp.416–429, 2008.
- [11] C. Ott, M.A. Roa and G. Hirzinger: "Posture and balance control for biped robots based on contact force optimization," 11th IEEE-RAS International Conference on Humanoid Robots, pp.26–33, 2011.
- [12] I. Park, J. Kim, J. Lee and J. Oh: "Mechanical design of the humanoid robot platform, hubo," Advanced Robotics, vol.21, no.11, pp.1305-1322, 2007.
- [13] J. Pratt and B. Krupp: "Design of a bipedal walking robot," Proceedings of the 2008 SPIE, vol.6962, 2008.
- [14] T. Takenaka: "The control system for the honda humanoid robot," Age and Ageing, 35-S2:24-26, 2006.
- [15] M. Vukobratovic and Y. Stepanenko: "On the stability of anthropomorphic systems," Mathematical Biosciences, vol.15, pp.1–37, 1972.



#### **Christian Ott**

received his doctoral degree in Automatic Control from the University of Saarland, Germany, in 2005. He was a visiting researcher at the University of Twente and worked for two years as a project assistant professor at the University of Tokyo. Cur-

rently he is working as a group leader of a Helmholtz Young Investigators Group at the Institute of Robotics and Mechatronics of the German Aerospace Center (DLR). His main research interests are the application of nonlinear control methods to robotic systems, force and impedance control, and control of humanoid robots.



#### Johannes Englsberger

is a research associate at the Institute of Robotics and Mechatronics, German Aerospace Center (DLR). He received his Diploma (equivalent to a M.Sc. degree) in Mechanical Engineering from Technical University of Munich (TUM) in 2009. His

research interests include bipedal locomotion control and the mechanical design of humanoids.



# Alin Albu-Schäffer

received the Ph.D. degree in Control Systems in 2002 from the Technical University of Munich. Since 1995 he is with the Institute of Robotics and Mechatronics at the German Aerospace Center (DLR). Since 2009 he is head of the Department

of Mechatronic Components and Systems. Additionally, he is a lecturer at the Technical University of Munich since 2007. His research interests include robot design, modeling, and control, nonlinear control, flexible joint and variable compliance robots, impedance and force control, physical human-robot interaction.



# Oliver Eiberger

received his Dipl. -Ing. degree in Mechanical Engineering from the Technical University of Munich (TUM) in 2000 and joined the German Aerospace Center (DLR) in the same year. His research interests include the mechanical design of torque con-

trolled robots and variable impedance actuators.



#### Maximo A. Roa

received his Ph.D. Degree in Robotics and Advanced Automation from the Technical University of Catalonia (UPC), Barcelona, Spain, in 2009. Currently, he is a Researcher at the Institute of Robotics and Mechatronics, German Aerospace Center

(DLR). Previously he worked as an R&D Specialist for Hewlett Packard, and also as a Researcher and Assistant Professor in the Department of Mechanical and Mechatronic Engineering, National University of Colombia. His main research interests include grasping and manipulation, mechanical hands, telemanipulation, and biped robots.